NASA DEVELOP National Program
Georgia – Athens

Spring 2024

Sarasota Climate

Monitoring Heat and Assessing Heat Vulnerability to Identify Locations for Heat Mitigation Efforts in Sarasota, Florida

DEVELOP Technical Report
March 29th, 2024

William Hadley (Project Lead)
Casmir Brown
Catherine Gallagher
Theresia Phoa

Advisors:
Dr. Marguerite Madden, University of Georgia (Science Advisor)
Joseph Spruce, Langley Research Center, Analytical Mechanics & Associates (Science Advisor)

Fellow:
Megan Rich (Georgia - Athens)

1. Abstract

The coastal county of Sarasota, Florida, is located within the humid subtropical climate region and experiences an average of 250 days of sunshine every year. The county has large, urbanized communities which are vulnerable to urban heat island (UHI) effects. These rapidly growing communities contribute to the increasing surface temperatures and placing more residents at risk of heat-related illness. In partnership with Sarasota County Sustainability, the Sarasota Climate team utilized Earth observation data from NASA Landsat 8 and Landsat 9's Thermal Infrared Sensors (TIRS), and the International Space Station's Ecosystem Spaceborne Thermal Radiometer Experiment on Space Station (ECOSTRESS) to model UHI effects within the county during the Summer for the last five years, 2019 to 2023. Data analysis with the Integrated Valuation of Ecosystem Services and Tradeoffs (InVEST) and Urban Heat Exposure Assessment Tempe 1.0 (UHEAT 1.0) models and within ModelBuilder produced maps that identified the land surface temperature (LST) variance within the county, the regions that are most susceptible to extreme heat, and areas least capable of mitigating the effects of UHI. The results revealed that heat intensity varies significantly across Sarasota County with the highest temperatures in the more developed western part of the county. Additionally, the team identified that there are at least three vulnerable communities that exist in high-heat regions, including North Sarasota, Venice, and North Port. These regions have an overlap between socioeconomic sensitivity and environmental hazard that indicate a high priority in future heat mitigation efforts.

Key Terms

Remote sensing, urban heat island, land surface temperature, Landsat, ECOSTRESS, InVEST, urban development, climate adaptation.

2. Introduction

2.1 Background Information

Urban areas are at particular risk from the effects of high temperatures, primarily because of the replacement of heat-mitigating natural landscapes with artificial blacktop and infrastructure that have lower albedo, causing them to retain heat during the day rather than dispel it. This phenomenon, known as the Urban Heat Island (UHI) effect, can make cities substantially hotter than the less developed land that surrounds them and can be hazardous to the health of city inhabitants (Nuruzzaman, 2015). A number of health problems stem from prolonged exposure to high temperatures including dehydration, heatstroke, and in serious cases, death. A meta-review (Faurie et al., 2022) analyzing and comparing 62 previous studies on heat vulnerability found that all three had substantial statistical associations with high-temperature events such as heatwaves. The direct heat illness, morbidity, and mortality increases by 18% for every increase of 1°C compared to the collective baseline.

Outside of environmental variables that contribute to UHI effects, demographic factors such as age, income, poverty and education levels, and minority status are crucial, along with population density and access to home amenities (namely air conditioning). These factors are central to creating a robust Heat Vulnerability Index (HVI) (Bao et al., 2015; Hansen et al., 2013). In high-mortality heat wave events, the main casualties belong to very specific demographic categories: during the 1995 Chicago heatwave, the majority of the over 700 inhabitants that died were elderly, impoverished, isolated, and without air conditioning (that they could afford to turn on) (Semenza et al., 1996). These same demographic groups also had the highest number of casualties from the 2003 European heatwave, which killed 14,800 in France alone (Bouchama, 2004). In addition to these factors, minority groups are likewise disproportionately vulnerable to heat hazards as they, along with the financially disadvantaged, are reportedly more likely to live in higher-temperature neighborhoods and ones that lack suitable air conditioning (Hansen et al., 2013).

Aside from causing human health issues, the UHI effect can damage both infrastructure and energy use, degrading environmental quality and causing electricity consumption to counteract rising temperatures on a short-term basis (Méndez-Lázaro et al., 2018). To protect city inhabitants and infrastructure, many small- and

large-scale governments with cities facing substantial heat threats are looking into mitigation efforts to counteract soaring temperatures. To do so, they must first identify areas that are particularly vulnerable to the UHI effect, on a physical (infrastructure) level as well as regarding the different demographic factors that make certain groups more vulnerable to heat hazards than others. Among these governments is that of Sarasota County, a region which has both significantly urbanized areas as well as consistently high summer temperatures.

Sarasota County is an area encompassing 556 square miles (1440 square kilometers) of land along the western coast of Florida (Figure 1). According to the US Census Bureau (V2023), it has a population of over 460,000 residents, almost 40% of which are 65 years old or older. The median household income within Sarasota County is around $77,000 per year (almost $3,000 more than the countrywide median, which is $74,580), with around 8.5% of the total population falling under the poverty line. Most of the year is spent in sunshine, and the county experiences a humid subtropical climate, both of which contribute to an overall risk of heat-related hazards, particularly in the summer.

Figure 1. Map of the study area, Sarasota County, Florida.

Sarasota has experienced a significant temperature increase starting from 1970, with average daytime temperatures rising by 2.6°F and nighttime temperatures by 5.9°F in summer (Figure 2; Climate Central, 2022). Observation data from the National Weather Service (NWS) Tampa provides appalling records on extreme heat events in Sarasota County. Since 2005, the county has seen 50 days categorized as extremely hot, that is when the heat index ('feel-like' temperature) going beyond 100°F. Last year in 2023, there were already 63 consecutive days surpassing 100°F and a whole week recording heat index above 110°F. What is more alarming is that climate projections from a Union of Concerned Scientists' study in 2019 suggest a potential escalation of this trend, with the occurrence of extremely hot days possibly reaching 131 by the mid-century (2030-2060s).

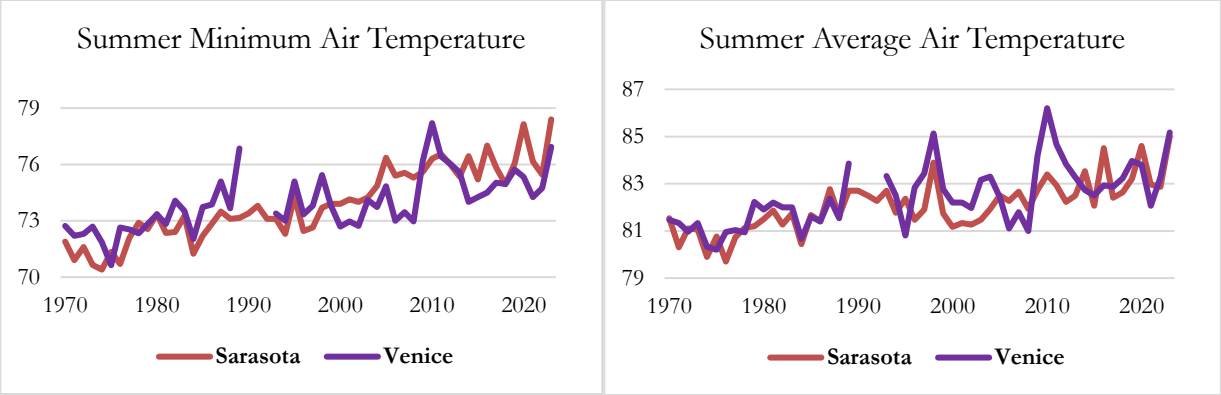

Figure 2. Average Air temperature trends in Sarasota County during Summer, minimum temperature (left) and maximum temperature (right) measured at the Sarasota-Bradenton Airport, representing northern part of Sarasota County, and Venice Municipal Airport, representing the southern part. *Data sources: NOAA Online Weather Data.*

The concern about the associated risks between climatological, health, and demographic factors in Sarasota County motivated county representatives to reach out to DEVELOP to help identify areas of risk to best determine mitigation efforts for the future; they requested that an HVI be constructed to aid county urban heat mitigation efforts. They particularly recognized the importance of factors like race and income in causing certain residential areas to be more susceptible to heat hazards than others, with two noteworthy areas in Sarasota – North Port and Newtown – as having human populations that include the at-risk groups mentioned.

2.2 Project Partners & Objectives

This project operates in conjunction with the government of Sarasota County Government and the University of Florida/Institute of Food and Agriculture Sciences (UF/IFAS) extension, who are interested in identifying the most heat-vulnerable areas within the county based on climatological and demographic data. The primary focus of this collaborative effort lies in public outreach, with the aim of providing crucial information to vulnerable residents in Sarasota County to help them navigate potential heat emergencies effectively. The heat vulnerability assessment conducted across summer months in Sarasota County from 2019 to 2023 will identify problematic areas and enable tailored mitigation efforts to address the unique needs of these communities, such as implementing tree-planting initiatives and establishing designated cooling centers. The project's final end products (Urban Heat Anomaly Map, Urban Heat Mitigation Potential Map, and HVI Bivariate Maps) will be reviewed by the partners to inform the development of education and mitigation plans that best cater to the constituents' requirements. Also, this project's outcomes will be disseminated across various departments within the county government. The GIS and Communication department will work on making the data accessible to the public through an interactive web map, while collaboration with the Sarasota County Health Department will aim at establishing a resolution focused on raising awareness about the impacts of extreme heat.

3. Methodology

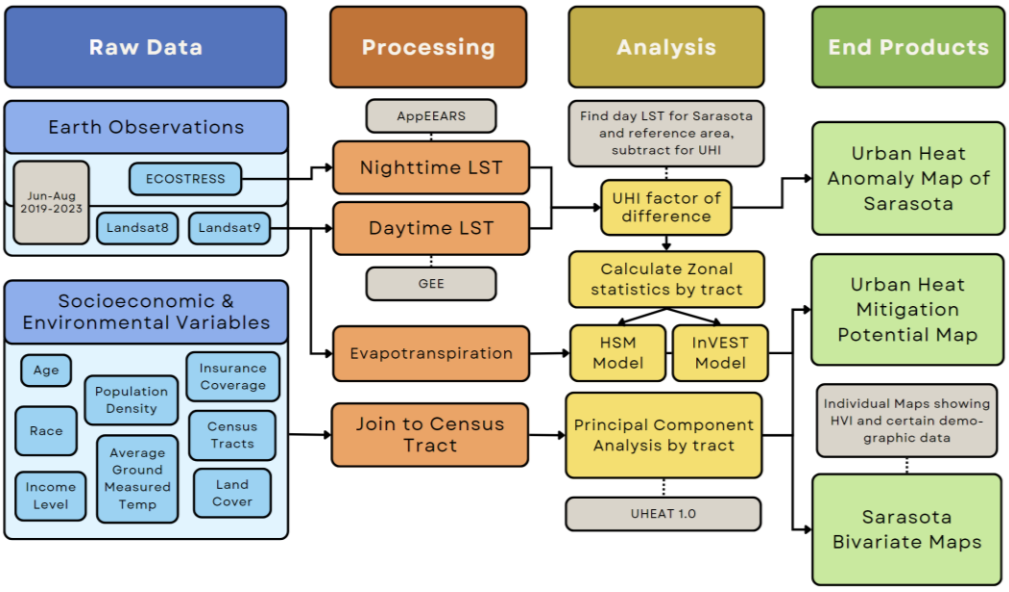

Figure 3. Sarasota County Urban Heat Island Monitoring and Assessment Workflow.

When determining appropriate extreme heat impact mitigation efforts and identifying a starting point, it is crucial to consider the knowledge about the specific area and the availability of data and archives. Though in-situ measurements are desirable for their precise information, these may not be widely accessible due to their high costs, ongoing maintenance requirements, and limited coverage in terms of space and time. Alternative approaches, such as synoptic remote sensing techniques, can be explored to address these limitations. These offer data for viewing and assessing large-scale heat hotspots and possibly enable the estimation of future conditions, providing a more comprehensive understanding of the impact of extreme heat.

The project consisted of the following four stages: GIS data collection, processing, analysis, and end products. First, the GIS data collection step involves determining which variables would be useful in UHI monitoring and assessment, which for this project included demographic data, such as race and age, remote sensing data, including land cover and average ground temperature, and the supplementary addition of health variables, which involves data such as asthma and Chronic obstructive pulmonary disease (COPD) cases. Then, the processing stage involves cutting down and formatting demographic data and creating LST and evapotranspiration maps, as well as connecting data to the actual census tracts for further investigation. Data analysis involves feeding the previous data into ArcGIS ModelBuilder and calculating zonal statistics using the products, as well as using a principal component analysis (PCA) to further identify areas of highest vulnerability. Finally, the end products stage involves using the information garnered from analysis to draw final conclusions and to create a series of maps, posters and other deliverables.

3.1 Data Acquisition

The data used for this project are listed in Table 1, 2, and 3. Table 1 outlines the NASA Earth observations and datasets used, Table 2 outlines ancillary datasets, and Table 3 describes the socio-economic variables the team used for analysis. The Sarasota Climate team obtained Landsat 8 Thermal Infrared Sensor (TIRS) Level 2, Collection 2, Tier 1 data through the Google Earth Engine (GEE) Catalog. Images with less than 20% cloud cover were selected for calculation of average daytime Land Surface Temperature (LST) using band 10 over the study period. To focus on the time when the urban heat island effect is most severe, the study period was restricted to the months of June, July, and August from 2019-2023. The team also obtained data from the International Space Station ECOsystem Spaceborne Thermal Radiometer Experiment on Space Station (ISS

ECOSTRESS) to calculate average nighttime LST as well as evapotranspiration. The ECOSTRESS data was obtained from the Application for Extracting and Exploring Analysis Ready Samples (AppEEARS) of the Land Processes Distributed Active Archive Center (Table 1; LP DAAC).

The evapotranspiration (ET) data that the team obtained from ISS ECOSTRESS was not utilized for this project due to numerous data gaps resulting from cloud coverage. Instead, the team acquired provisional actual evapotranspiration product, accessible only through the USGS Earth Resources Observation and Science (EROS) Science Processing Architecture (ESPA) On-demand Interface (https://espa.cr.usgs.gov/). Accessing this data required the preparation a standard text document (a.*txt* file) containing Landsat OLI data filenames. Our team selected the date of 22nd August 2023 path 016 row 041 for reference input of InVEST model because of the minimal cloud cover (6%) on the Landsat data from that date.

Table 1
List of Earth Observations and remotely sensed imagery used in data analysis.

Platform / Program	Sensor	Product ID	Purpose	Dates Used	Acquisition Method	Spatial Resolution
Landsat 8	OLI/TIRS	LANDSAT/LC08/C02/T1_L2	Daytime LST and albedo,for InVEST model.	June 1st – August 31st of 2019–2023	GEE Catalog	30-meter
Landsat 9	OLI-2/TIRS-2	LANDSAT/LC09/C02/T1_L2	Daytime LST, albedo, and provisional evapotranspiration (ETa) for InVEST model.	June 1st – August 31st of 2019–2023	GEE Catalog	30-meter
ISS	ECOSTRESS	ECO2LSTE.001	Nighttime LST	June 1st – August 31st of 2019–2023	AppEEARS	70-meter

To model heat mitigation using the Integrated Valuation of Ecosystem Services and Tradeoffs (InVEST) Urban Cooling Model, the team also accessed various ancillary datasets to use as inputs. Land cover data was acquired from the United States Geological Survey (USGS) National Land Cover Database (NLCD). The team accessed tree canopy data from the National Oceanic and Atmospheric Administration (NOAA) Coastal Change Analysis Program (C-CAP), building footprint polygons from Sarasota County, and reference evapotranspiration (ET_0). Finally, reference evapotranspiration (ET_0) that are required for Crop coefficient (K_c) to represent biophysical properties was acquired using the Mapping Evapotranspiration at high Resolution with Internalized Calibration (METRIC) method available through GEE, which is called Earth Engine Evapotranspiration Flux (EE-FLUX). EE-FLUX is developed and managed by the consortium of University of Nebraska-Lincoln, Desert Research Institute, and University of Idaho (Table 2).

Table 2
List of ancillary datasets.

Parameter	Provider	Purpose	Observation Period	Source	Resolution
Land Use/ Land Cover	USGS	Input for InVEST model	2021	USGS NLCD	30-meter
Tree canopy	NOAA	Input for InVEST model	2022	NOAA C-CAP	1-meter
Building footprint	Sarasota County	Input for InVEST model	2021	Sarasota County GIS Portal	Individual building structure
Reference Evapotranspiration (ET_0)	Consortium of University of Nebraska-Lincoln, Desert Research Institute and University of Idaho	Crop coefficient (Kc) calculation, input for InVEST model	August 22nd 2023	METRIC EE-FLUX	30-meter

The team accessed socio-economic and health variables for every census tract in Sarasota County to investigate the relationship between vulnerable populations and extreme heat. Socioeconomic variables were accessed from the Census Bureau's American Community Survey (ACS), and the health variables were accessed from the Center for Disease Control and Prevention (CDC) PLACES program (Table 3).

Table 3
List of socio-economic and health variables used in the analysis.

Dataset	Resolution	Date	Source
Population density	Census tract	2018-2022	American Community Survey (ACS) (NHGIS)
Percent of population under 5 years old			
Percent of population over age 65			
Percent of population that are non-white			
Percent of population that are non-citizens			
Percent of population below the poverty level			
Percent of population that speaks limited English			
Percent of households with no car			
Percent of population without health insurance			
Percent of population (18-64) that has a disability			
Percent of population (16+) that are unemployed			
Percent of population living alone			
Asthma patients	Census designated places	2019, 2020	CDC PLACES: Local Data for Better Health
People with Coronary Heart Disease			
People with obesity			
Stroke patients			

People with high blood pressure			
People with diabetes			
Chronic Obstructive Pulmonary Disease patients			

3.2 Data Processing

3.2.1 *Land Surface Temperature*

When accessing daytime land surface temperature (LST) data from Landsat 8, the team first filtered any pixels that were tainted by the presence of clouds or cloud shadows using the Landsat collection 1 level 1 Quality Assessment band containing information on the usability of pixels within a Landsat scene. To do this, the team developed a GEE script to classify and exclude likely cloud and cloud shadow-dominated pixels. The team then averaged the remaining cells across all dates in GEE to generate an average summer daytime LST map of Sarasota County for the years 2019 – 2023. The team converted the original temperature retrieval in degrees Kelvin to degrees Fahrenheit.

The team downloaded ECO2LSTEv001 datasets to calculate nighttime LST and filtered the images for nighttime hours. Similarly to Landsat images, the quality bands in the ECO2LSTEv001 were used to identify and remove cloudy or low-quality pixels. Following masking and filtering these low-quality pixels, the team calculated the mean LST of each pixel across the study area to calculate an average summer nighttime LST map of Sarasota County for the years 2019 – 2023. The entire ECOSTRESS was processed using Python programming language in Microsoft Visual Studio Code. The original unit for the LST is Kelvin, so the team converted it into Fahrenheit after both daytime and nighttime LST data were exported to ArcGIS Pro 3.2.2.

3.2.2 *Landcover*

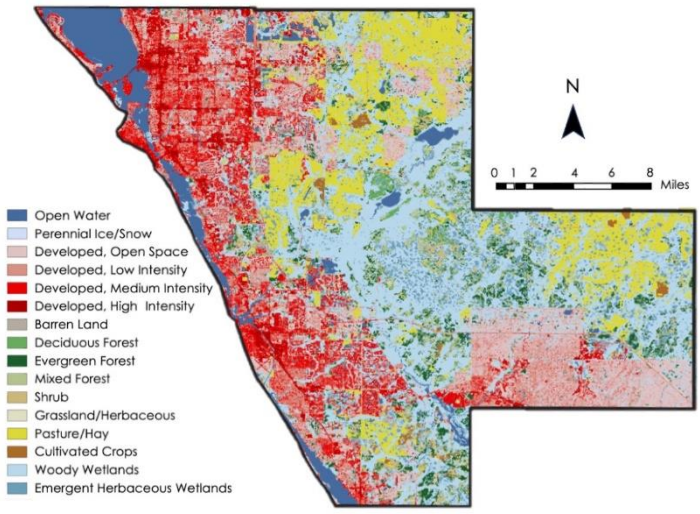

Figure 4. 2021 NLCD land cover categories for Sarasota County.

The team incorporated the 2021 NLCD (Figure 4) into a Habitat Suitability Model (HSM) made in ModelBuilder in ArcGIS Pro. The HSM model is frequently used to identify optimal locations for specific purposes, such as implementing heat mitigation measures in this case. For this model, the team downloaded the data from the USGS website, added it to ArcGIS Pro, and projected it into World Geodetic System (WGS 1984). Then, using extract by mask, the team cut down the NLCD file to the size of the Sarasota County shapefile. Next, the team edited the new NLCD layer using the reclassify tool, narrowing down the original categories under four new ones: Developed, Low Intensity (Open Space/Developed, Low Intensity/Barren Land); Developed, Medium Intensity; Developed, High Intensity; and Non-Developed,

which combined all other categories together. This reclassified version is the one that was included in the land cover submodel of the HSM.

For our analysis using the InVEST model, the team also incorporated another dataset, NOAA C-CAP 2022. This dataset allowed us to examine the distribution and characteristics of land cover types in detail. Vegetated areas play a crucial role in moderating temperatures and enhancing cooling effects within urban environments. Yet, sourcing high-resolution data that accurately captures the intricate details of vegetation cover has posed a challenge. This difficulty persists even when considering established datasets like the NLCD.

The latest version of NOAA C-CAP data has been conveniently aggregated into canopy cover and impervious surfaces. This simplifies the team's workflow, as they can directly apply zonal statistics in ArcGIS Pro to calculate averages from individual pixels and determine the percentage of canopy cover and impervious surfaces within specific census tracts in Sarasota County (Figure 5a-b).

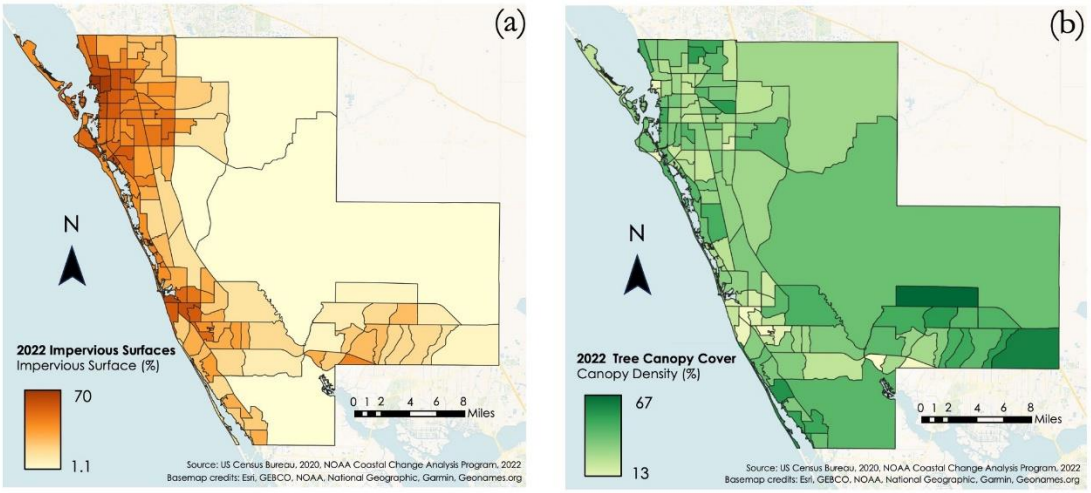

Figure 5. Derived (a) impervious surfaces and (b) tree canopy cover percentages, aggregated by census tract.

3.2.3 *Biophysical Properties*

One essential input of the InVEST model is the biophysical properties table, comprising factors such as crop coefficient (K_c), albedo, shade ratio, and building intensity. In this model, K_c represents the ratio of observed evapotranspiration for specific land cover under identical conditions. Typically, K_c is calculated using potential evapotranspiration (ET assuming ideal water supply) as the numerator and ET_0 as the denominator (Eq. 1; Allen et al., 1998). However, without potential ET data, the team attempted to substitute it with Landsat Provisional Actual ET data. As for the ET_0, the team utilized a downloadable raster layer from the METRIC EE-FLUX interface, and the following equation is to compute K_c:

$$K_c = \frac{ET_a}{ET_0} \qquad \text{(Eq. 1)}$$

In the albedo calculation, Landsat 8 OLI digital numbers (DNs) are transformed into Top of Atmosphere (TOA) reflectance using a simplified method from the Yale Center of Earth Observation. This method adapts the algorithm formulas developed by Liang (2001) and later improved by Smith (2010) using DNs from five reflectance bands (Red, Blue, Near Infrared, Shortwave Infrared 1, and Shortwave Infrared 2) to produce shortwave albedo α_{short}. The formula is applied using the mathematical function in GEE, expressed as:

$$\alpha_{short} = \frac{0.356_{blue}+0.130_{red}+0.373_{NIR}+0.085_{SWIR}+0.072_{SWIR\,2}-0.018}{1.016} \quad \text{(Eq. 2)}$$

For the shade ratio and building density inputs, the team extracted values by applying zonal statistics in ArcGIS Pro on the 2022 NOAA C-CAP canopy cover and impervious surface datasets. These datasets are overlayed with the NLCD grid, which delineates boundary areas of each land cover type. This process allowed the team to calculate the proportion of shaded areas and density of built structures within each grid cell since C-CAP datasets have higher spatial resolution than NLCD. Table 4 is the biophysical properties table for the InVEST model input, derived specifically for Sarasota County.

Table 4
InVEST Urban Cooling Model Biophysical properties table

No	lucode	Description	Shade	Kc	Albedo	Green_area	building_intensity
1	11	Open Water	0	0.59	0.03	1	0
2	21	Developed, Open Space	0.47	0.45	0.07	0	0.1
3	22	Developed, Low Intensity	0.36	0.37	0.08	0	0.28
4	23	Developed, Medium Intensity	0.24	0.32	0.1	0	0.44
5	24	Developed, High Intensity	0.14	0.26	0.14	0	0.65
6	31	Barren Land	0	0.38	0.12	0	0.09
7	41	Deciduous Forest	0.12	0.41	0.05	1	0
8	42	Evergreen Forest	0.64	0.5	0.05	1	0
9	43	Mixed Forest	0.43	0.46	0.05	1	0
10	52	Shrub/Scrub	0.32	0.4	0.06	1	0
11	71	Herbaceous	0.31	0.45	0.06	1	0.05
12	81	Hay/Pasture	0.13	0.45	0.07	1	0
13	82	Cultivated Crops	0.15	0.49	0.07	1	0
14	90	Woody Wetlands	0.63	0.54	0.05	1	0
15	95	Emergent Herbaceous Wetlands	0.19	0.5	0.05	1	0

3.2.4 *Demographic data*

The team acquired demographic information from the American Community Survey (from the US Census and downloaded through IPUMs NHGIS as a proxy) for the years 2018 through 2022. The demographic variables are as follows: population density, percent under 5 years old, percent over 65, percent non-white, percent living alone, percent disabled, percent over 16 that are unemployed, percent non-citizens, percent with no health insurance, percent who spoke limited English, percent below the poverty level, and percent with no car. Each of these individual Excel files was added to ArcGIS Pro and joined to copies of the shapefile of census tracts sourced from the US Census. From the total numbers, the team then calculated the percent of the overall population and symbolized the census tracts with graduated colors & natural breaks (for Figure 6 and Figure C).

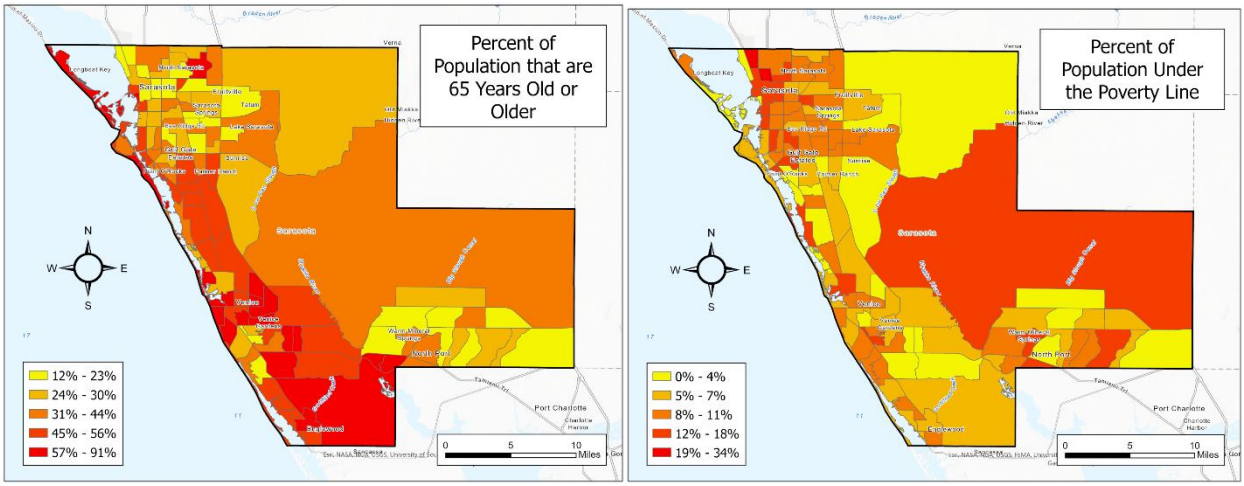

Figure 6. Two key demographic breakdowns in Sarasota County, Fl.: percent of population that is 65 or Older and that is under the Poverty Line.

3.3 Data Analysis

3.3.1 *Diurnal Land Surface Temperature Difference*

When assessing the impact of extreme heat on the urban environment, examining diurnal temperature variations is analogous to investigating the area's thermal dynamics. Temperature changes between night and day provide insights into places that were highly exposed to extreme heat, the mechanisms contributing to prolonged warmth in specific locations, and the impact of various surface types, such as concrete or green spaces, on thermal conditions. In creating diurnal LST difference maps, the team used ArcGIS Pro to subtract nighttime temperature values from daytime temperature values. This method results in a spectrum of outputs: warming areas (positive values), cooling areas (negative values), or areas where LST remains unchanged. To enhance the precision of our analysis, the team implemented the Con tool to eliminate data that display warming trends, where the difference between nighttime LST is less than daytime LST.

3.3.2 *InVEST Urban Cooling Model*

Integrated Valuation of Ecosystem Services and Tradeoffs (InVEST) is an open-source software developed by Stanford University's Natural Capital Project that provides a variety of models, including Urban Cooling (Natural Capital Project, 2024). The model constructs heat mitigation output based on biophysical parameters such as evapotranspiration and albedo, and it also weighs the impact of parks or other cooling islands (Zawadzka et al., 2021). Several DEVELOP projects have applied the model to several cities in the US, such as Fairfax, Yonkers, and Wichita (Holloway et al., 2021; Walechka et al., 2021; Ghosh et al., 2022).

To investigate what communities of Sarasota County are most and least mitigated against the effects of UHI, the team utilized the InVEST Urban Cooling Model's Cooling Capacity Index (CCI) output. CCI is a unitless value that simulates the ability of a region of the study area to cool itself, and the model considers shade, evapotranspiration, albedo, and distance from nearest greenspace in its calculations. To generate this, the team input the landcover and evapotranspiration datasets previously accessed into the InVEST application along with a spreadsheet describing the biophysical properties of each landcover type. The team ran the models that account for both the daytime CCI and the nighttime CCI, as specified by the UHI effects calculated in the LST anomaly maps.

3.3.3 *ArcGIS Model Builder*

Another avenue of analysis involved combining demographic, land cover, and climatological remote sensing data – health data was excluded because its nature as centroid data would have thrown off spatial analysis – in order to assess collective vulnerability to heat. Data was downloaded from the sources mentioned above and

added to an ArcGIS Pro project. From there, a new ModelBuilder tab was opened, with the Environments section tailored to create an end raster with a 30-meter resolution, much like that of the NLCD. Each of the three groups of data was assigned to its own submodel: all demographic data was then converted using polygon to raster, each of which was then fed through rescale by function (using ArcGIS Fuzzy MS Large classification) to split each into a 1-10 scale. Each of the rescales was then recoalesced using weighted sum and then weighted into the final submodel layer according to their prevalence in similar heat vulnerability indexes and their magnitude of influence in hazard casualties (Table 5), both according to the literature review (Bao et al., 2015; Benmarhnia et al., 2015; Bouchama, 2004; Faurie et al., 2022; Ghosh et al., 2022; Harlan et al., 2014; Hansen et al., 2013; Méndez-Lázaro et al., 2018; Semenza et al., 1996; Walechka et al., 2021; and Yardley et al., 2011*).*

The next submodel involves land cover. Since all of the land cover data existed on the same raster – the 2021 NLCD layer – the only operations that were required were the Reclassify tool, in order to simplify the many land cover types into four more compact levels of development: non-developed; developed, low intensity (including open space/barren); developed, medium intensity; and developed, high intensity. From there, the rescale tool broke down the development raster into a 1-10 scale of intensity (likewise Fuzzy MS Large). The final submodel involved three types of climatological data: daytime LST, nighttime LST, and evapotranspiration. All three raster layers – after zonal statistics had been calculated – were rescaled by function and then likewise put weighted due to their influence on heat risk from 1 (low) to 3 (high). Lastly, the three submodels are combined through one final weighted sum (according to Table 5.1) into the overall Heat Vulnerability Model (Figure 9). All variable weights and designations can be found in Table 5. The overall breakdown of the final vulnerability model can be seen in Figure D.

Table 5
Details of demographic modeling.

Variable	Weight	Source	Year
Population Density	2	US Census (IPUMS NHGIS)	2018-2022
% Under 5 Years Old	1		
% Over 65 Years Old	3		
% Non-White	2		
% Disabled	2		
% Unemployed (16+)	2		
% Not a citizen	3		
% No Health Insurance	2		
% Limited English	2		
% Below Poverty Level	3		
% Living Alone	3		
% No Car	2		
Non-Developed	1	National Land Cover Database	2021
Developed, Low Intensity/Open Space/Barren			
Developed, Medium Intensity			
Developed, High Intensity	10		
Nighttime LST (Average)	3	ISS ECOSTRESS	2019-2023
Daytime LST (Average)	3	Landsat 8 and 9	

Evapotranspiration	2		

Table 5.1. Submodel Weights	
A	*1*
B	*2*
C	*2*

3.3.4. *Principal Component Analysis*

When conducting UHI assessments, analyzing data with numerous variables often poses challenges related to multidimensionality. Principal Component Analysis (PCA) is a powerful statistical method for addressing these challenges by reducing the dimensionality of the data, simplifying interpretations, and identifying the critical factors influencing extreme heat exposure and vulnerability in a comprehensive manner (Conlon et al., 2020). Using this quantitative approach, the team effectively categorized areas by integrating 16 variables (5 environmental and 11 socioeconomic), as listed in Figure 10, to establish a comprehensive score per census tract. PCA facilitated grouping highly correlated variables into principal components, thereby revealing the maximum variability within the dataset. Notably, significant descriptive power was wielded by variables within the first principal component, while subsequent components demonstrated diminishing explanatory capacity.

The DEVELOP Fall 2020 Tempe Urban Development II team initially created a script named UHEAT 1.0 (Urban Heat Exposure Assessment Tempe 1.0) in R programming language for data preparation, PCA analysis, visualization of variable loadings, and heat exposure scoring. Subsequently, the script was retrieved from NASA DEVELOP GitHub repository (https://github.com/NASA-DEVELOP/UHEAT/tree/main) and modified in Rstudio 4.3.3 to conform with the specific variables of interest for the Sarasota Climate team. Prior to PCA analysis, the input variables were standardized into Z-scores for data comparability. The team then proceeded to create Heat Exposure scores by analyzing the PCA findings, which involved assigning numerical values to assess the impact of heat on different geographic areas in Sarasota County. This process included calculating PCA scores for every factor and neighborhood. The team looked at various aspects, like temperature and demographic data, to gauge the level of heat exposure in each census tract. By combining all these scores, the team created a single overall score for each area. This helped the team quickly identify which neighborhoods are most at risk from heat-related issues.

3.3.5 *Cumulative Heat Vulnerability Index*

This project was conducted to provide a foundational reference for urban heat adaptation and mitigation that facilitates informed decision-making to address heat-related vulnerabilities in the community. The team proposed the development of an additional cumulative index to understand model outputs and streamline decision-making processes holistically. This index aims to efficiently identify high-priority spots while ensuring model consistency. By reducing the number of high-priority areas to the smallest feasible quantity, decision-makers can effectively allocate resources and implement targeted interventions.

Drawing upon a study by Reid et al. (2009), the team derived overall heat vulnerability community determinants. To ensure comparability and ease of analysis, the team computed the average of all model results using zonal statistics in ArcGIS Pro, consolidating them into a single value for each census tract. Subsequently, the cumulative heat vulnerability index was formulated. Each original model score was initially normalized to achieve a mean of 0 and a standard deviation of 1, called the Z-score. After that, the Z-scores were categorized into six groups based on standard deviations to enhance clarity and minimize the impact of outliers. These categories were assigned a final score ranging from 1 to 6, with 1 indicating the lowest vulnerability and 6 denoting the highest. Considering a limited understanding of nonlinear relationships, the team presumed linear associations between models and accorded equal importance to each. Finally, the team

generated a cumulative heat vulnerability index for every census tract by summing their final scores, and it will be called the Heat Mitigation Priority, signifying the priority of mitigation efforts.

4. Results & Discussion

4.1 Analysis of Results

4.1.1 LST and Diurnal LST Difference

Using LST data obtained from Landsat 8 OLI/TIRS, Landsat 9 OLI-2/TIRS-2, and ISS ECOSTRESS, the team produced a map illustrating both typical daytime (as seen in Figure 7a) and nighttime (depicted in Figure 7b) surface temperatures during the summer period spanning from 2019 to 2023. Through this analysis, it became apparent that daytime temperatures varied between 61 to 116°F, revealing discernible distinctions between urban and rural regions. Conversely, nighttime temperatures appeared relatively uniform, ranging from 69 to 93°F.

In Figure 7c, the map illustrates the extent of cooling that occurs during the nighttime hours. Interestingly, it was observed that urban hotspots, such as the Northwestern area of Sarasota County, exhibited a more rapid cooling process than anticipated. Areas close to water bodies or along the coastlines experienced minimal cooling, attributed to the higher heat capacity of water compared to land surfaces. The observed phenomenon may be attributed to the high albedo values depicted in Figure 7d, representing the fraction of solar radiation reflected by the surface. This suggests that these surfaces do not retain heat for prolonged periods, contributing to the quicker cooling observed in certain urban areas and the contrasting minimal cooling near water bodies.

The likelihood of a higher albedo value might be from various factors, including dense canopy cover (Figure 5b) and buildings equipped with light-colored roofs. Surfaces with lighter coloration tend to reflect a greater amount of solar radiation (NASA, 2019). Such features contribute to an increased albedo, influencing the overall reflectivity of the surface and subsequently impacting heat retention and cooling dynamics in the surrounding environment.

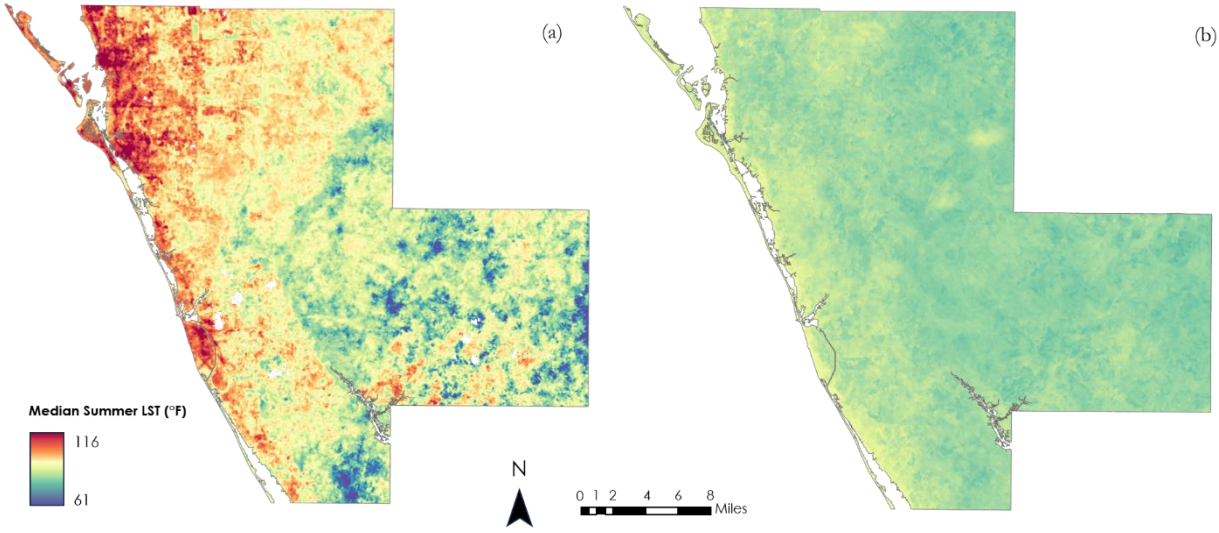

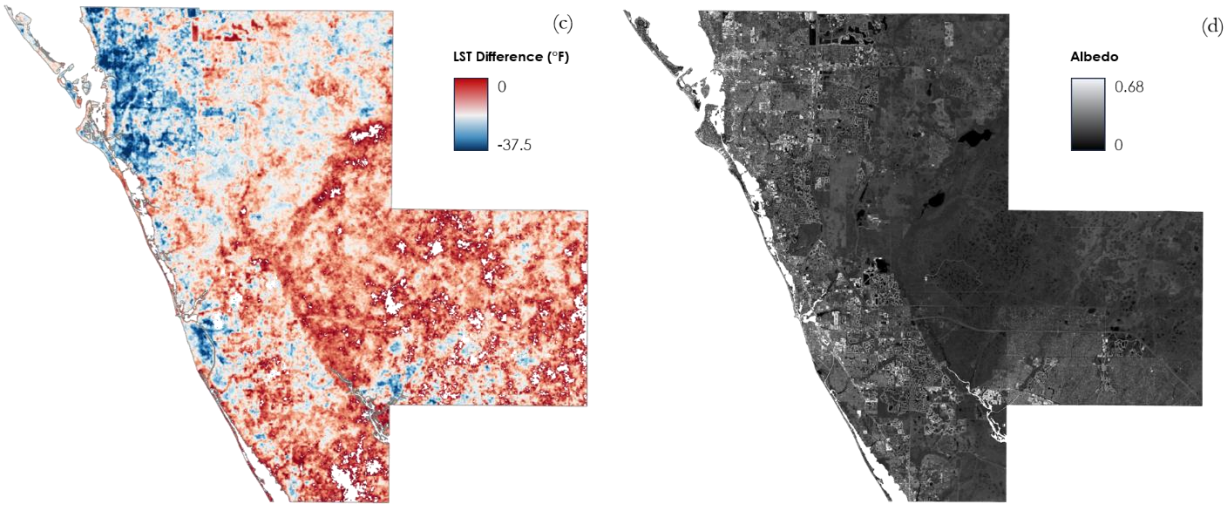

Figure 7. (a) Median Daytime LST, (b) Median Nighttime LST, (c) LST difference (Nighttime LST-Daytime LST), and (d) Average surface albedo in Sarasota County throughout Summer 2019-2023.

4.1.2 Cooling Capacity Index

The team generated a Cooling Capacity Index using the InVEST urban cooling model. This model, which considers shade, evapotranspiration, albedo, and distance from cooling green spaces, outputs a unitless value approximation of the ability of a location to dissipate heat and ranges from 0 (little ability to dissipate heat) to 1 (significant ability to dissipate heat). As shown in Figure 8, this index varies significantly across the county and largely mirrors the daytime land surface temperature map of the county, showing the western, developed region of the county retaining significantly more heat than the eastern, more vegetated region.

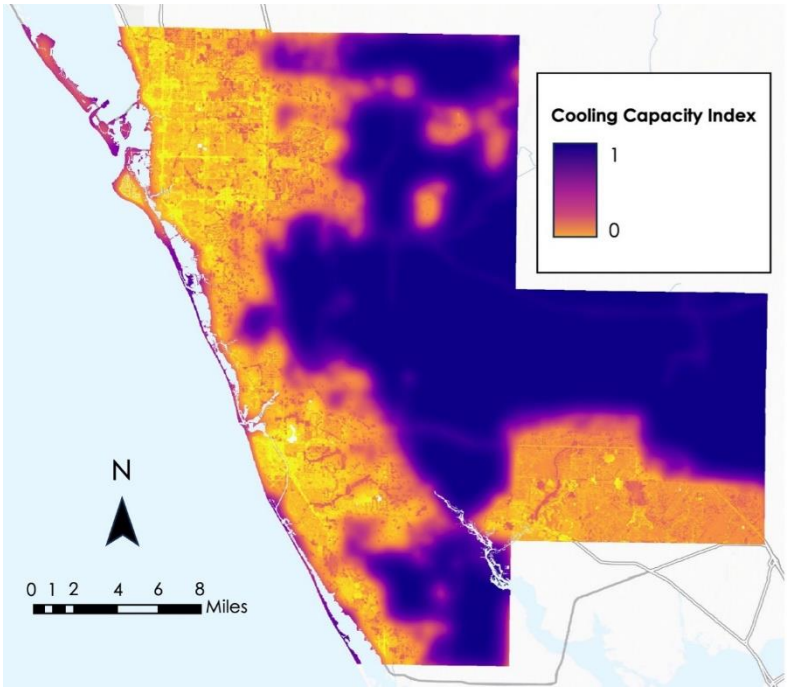

Figure 8. Sarasota County's cooling capacity index, from 0 (low ability to cool) to 1 (high ability to cool).

4.1.3 Heat Vulnerability

The trend shown in Figure 9 depicts vulnerability favoring the coastline of Sarasota County, with the areas of highest potential risk being parts of Western and Northern Sarasota City, Venice, Englewood, and North Port. Out of the three main areas with the highest vulnerability, Northern Sarasota is the one with the overall highest risk based on the variables included in the model; with daytime LST temperatures up to 116°F and nighttime temperatures of upwards of 93°F, along with high percentages of populations with vulnerable demographic factors – including Sarasota residents who are under the poverty line or unemployed – and some of the most highly-developed land in the entire county. Census tract 2, for example, is the most singularly vulnerable tract in the whole of Sarasota County according to the combined model and is located in the Northwestern part of the city and surrounded by similar patches of high vulnerability. Venice is the area with the next highest level of overall vulnerability – though in this instance, age demographic factors play a higher role that in North Sarasota or North Port, with a substantial number of residents being 65 or older – likewise clustered towards the west along the coastline. Englewood and North Port similarly have high vulnerability due to age demographics in conjunction with socioeconomic variables and low albedo land cover.

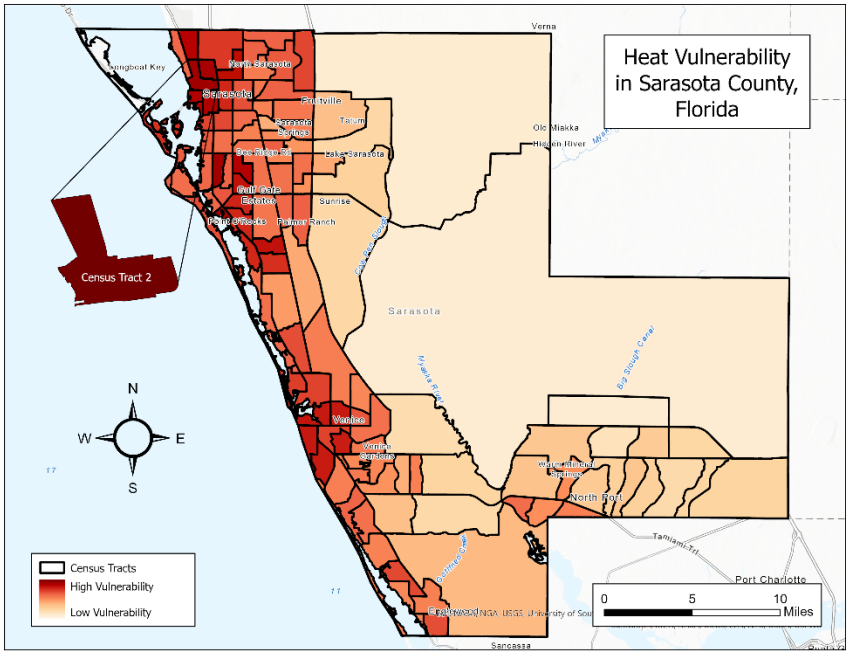

Figure 9. Heat vulnerability across Sarasota County.

4.1.4 Heat Exposure

The PCA ran on the selected 16 variables by the Sarasota Climate team (Figure 10) applied specific criteria, retaining only components with eigenvalues surpassing one and explaining at least 80% of the data variance. This process yielded four principal components (PCs). Collectively, these components elucidate 69% of the variances observed in the dataset, with PC1 and PC2 accounting for 42% of the total variations. Notably, PC1 and PC2 showcase significant explanatory power, particularly in relation to daytime Land Surface Temperature (LST). Key contributors to these components include the percentage of impervious surfaces, canopy cover, albedo, and total population, as evidenced by their strong loadings on daytime LST. While the third PC explains only 15% of the total apparent variance, its interpretation unveils an alternative perspective. Here, vulnerability assessment based on Nighttime LST, percentage of the population aged 65 and over, and occupational status, such as individuals not in the labor workforce, emerge as pertinent indicators.

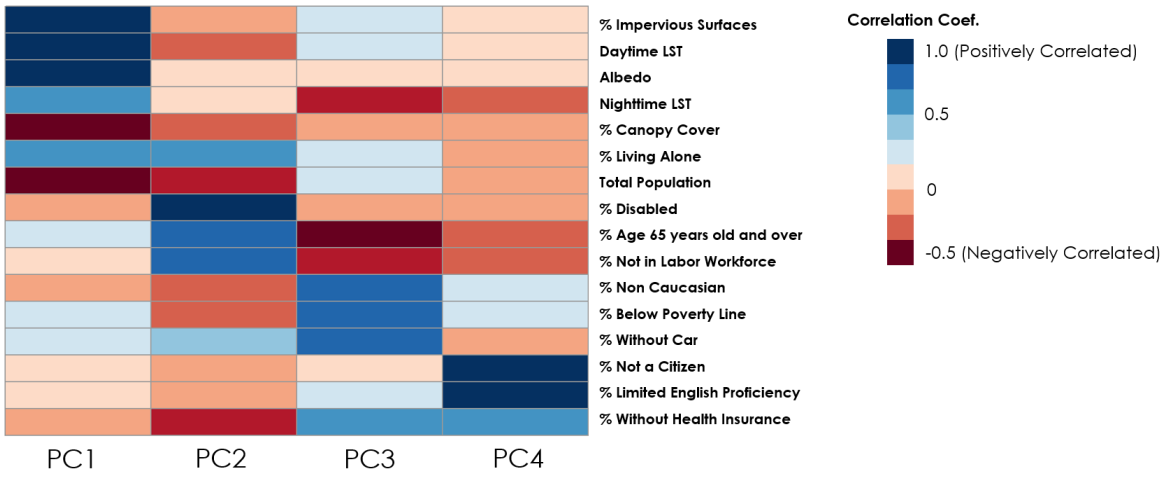

Figure 10. Principal Component Analysis variable loadings correlation matrix.

To quantify heat exposure patterns in Sarasota County, the team used a PCA to generate Heat Exposure scores. These scores were then joined into a geographical map using ArcGIS Pro, with the Quantile approach meant to classify census tracts based on heat exposure intensity, which ranged from low to high. The classification revealed 24 census tracts with High Heat Exposure, with a significant concentration in metropolitan regions such as Sarasota, Venice, and North Port (Figure 11). These clustering patterns could be attributable to factors such as higher population density and larger data values, indicating a link between urbanization and increased heat vulnerability.

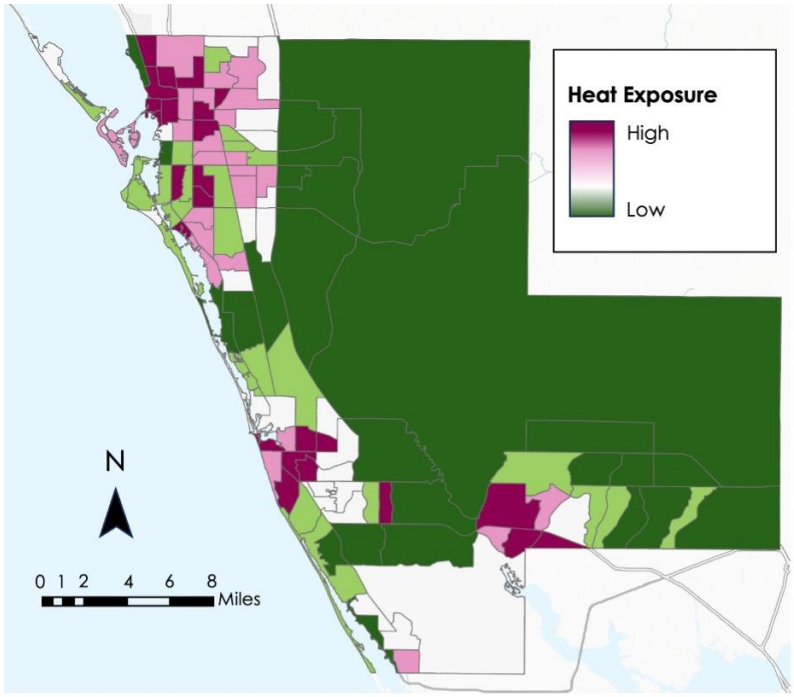

Figure 11. Heat exposure across Sarasota County aggregated by Census tract.

4.1.5 Heat Mitigation Priority

A Heat Mitigation Priority Map (Figure 12) was created to evaluate the outcomes of three distinct models, each distinguished by its unique characteristics and methodologies. The Cooling Capacity Index model prioritized environmental conditions and was generated utilizing prebuilt InVEST software, focusing on

identifying areas with inherent natural cooling potential. Second, the Heat Vulnerability model, constructed through ArcGIS Pro ModelBuilder, employed a weighted sum methodology grounded in Spatial Analysis to assess various socio-environmental factors contributing to vulnerability based on literature reviews. Third, the Heat Exposure analysis, facilitated by a PCA, integrated both statistical and spatial analyses to understand the spatial distribution of heat exposure across the region.

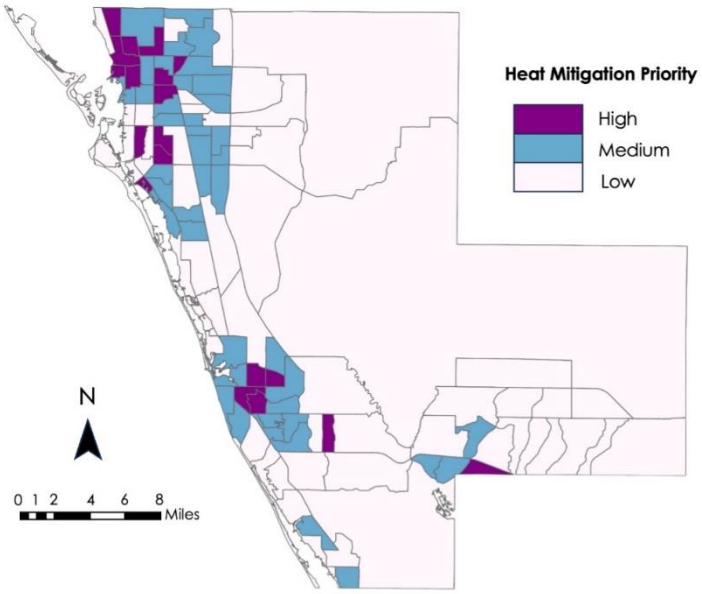

Figure 12. Cumulative Heat Vulnerability Index for Sarasota County, aggregated by Census tract.

As seen in Figure 13, North Sarasota is, by far, the area with the highest overall vulnerability to heat hazards and therefore that which also requires primary mitigation priority. It contains multiple census tracts that both have high rates of unemployment and poverty while also having average daytime LST of over 100 degrees Fahrenheit, making them particularly vulnerable to heat hazards.

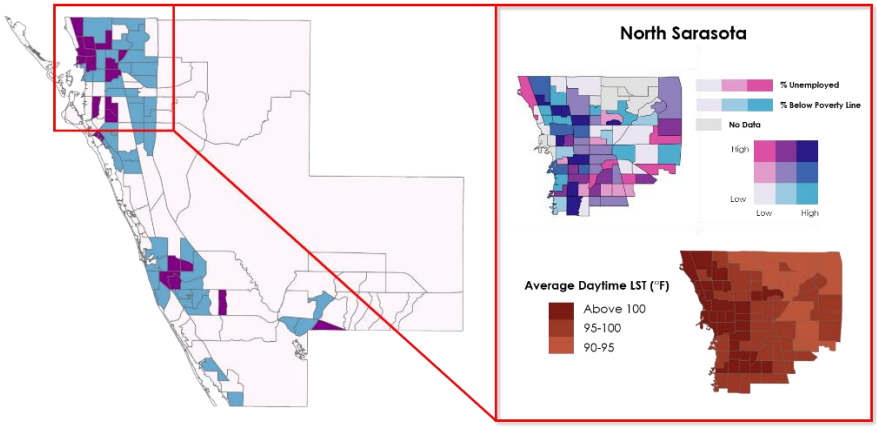

Figure 13. North Sarasota Socioeconomic Profile and Average Summer 2019-2023 Daytime LST.

Venice (Figure 14) has a high number of residents that are 65 years or older, with a few of these communities also existing below the poverty line, making Venice a notable intersection between physical demographic risks (age) and socioeconomic ones. While not as hot during the day overall as in North Sarasota, daytime LST in the summer in Venice is still dangerously high given the demographic risks present.

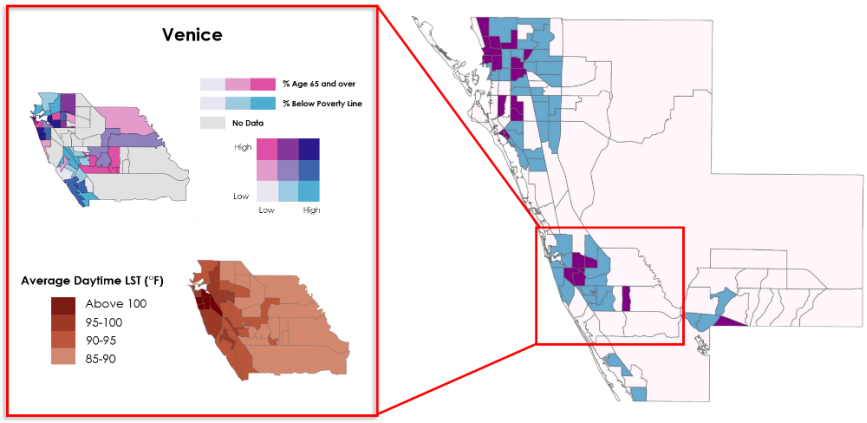

Figure 14. Venice Socioeconomic Profile and Average Summer 2019-2023 Daytime LST.

With a combination of similar demographic risks to North Sarasota (unemployment rates, poverty, etc.), though there are also physical risks present as well (the census tract with the highest elderly population by percent), North Port is the final area towards which heat mitigation ought to be directed with priority as shown in Figure 15. While average daytime LST is lower in much of North Port than in Northern Sarasota City or Venice, it is still higher than many other parts of the county (in combination with demographic risks and land cover factors).

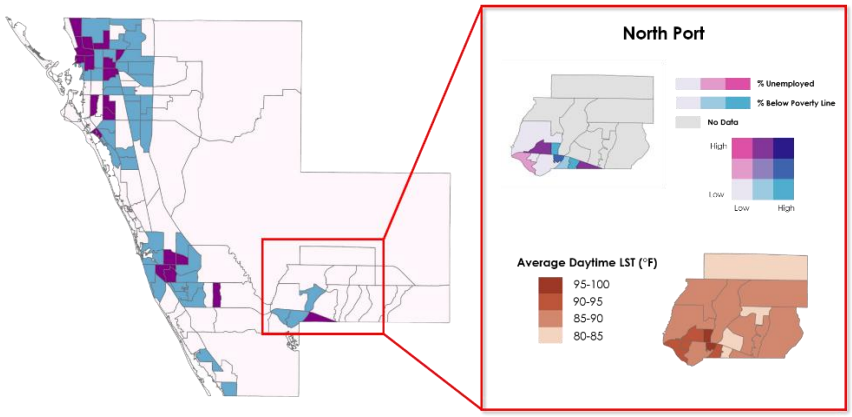

Figure 15. North Port Socioeconomic Profile and Average Summer 2019-2023 Daytime LST.

4.1.6 Demographic Data

A demographic breakdown of the locations of vulnerable populations, available in Appendix C, shows that the pattern of vulnerability across Sarasota County shifts significantly depending on what type of demographic information is being mapped. The highest population density is centered around the City of Sarasota, which has the second highest overall population of the county (only after North Port, which had a medium population density). There is a large swath of census tracts with very high population densities – measured as number of people per square mile – in North Sarasota. Patterns differ depending on whether they are considered to contribute to physical risk to heat hazards versus social risks. For example, demographic factors associated with age - such as being under five, over 65, or disabled – are clustered largely in the southern part of the county, while most other variables – which focus on social determinants such as race or language capacity – are centered mostly in the northeast, particularly in North Sarasota though they also are prominent in North Port. Overall, North Sarasota and North Port both reflect high percentages in almost every category. In fact, in some areas of North Sarasota, the percentage of non-white inhabitants is

almost 95 percent, while in other tracts, particularly in the southwest and along the coasts, that number is almost zero. Areas with the highest percentage of people under the poverty line (up to a third of the total) include North Sarasota, North Port, and the large section of land in the central/eastern section of the county.

4.2 Limitations

4.2.1 Evapotranspiration

Due to frequent cloud cover in the Landsat provisional evapotranspiration product, the team only used a single date of data (22nd August 2023) path 016 row 041, as an input for the InVEST urban cooling model. The team assumed that this date was representative of the typical behavior of evapotranspiration in the county, but average evapotranspiration may differ significantly.

4.2.2 Health Data

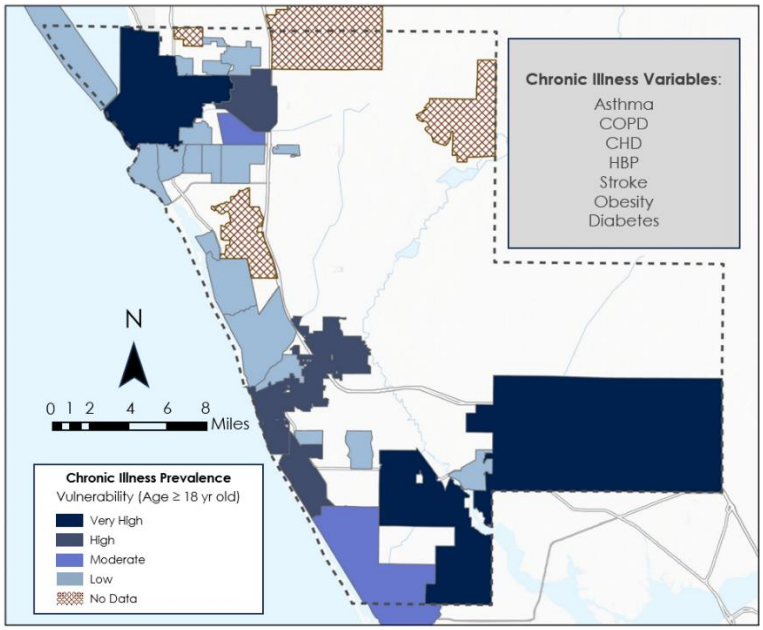

Figure 16. Combined chronic illness prevalence for asthma, COPD, CHD, HBP, stroke, obesity, and diabetes across Sarasota County by Census-designated place. Prevalence by disease is available in Appendix B.

Initially, the team had expected to incorporate health data into the analysis of heat vulnerability. Though this data was available through the CDC Places tool, it was aggregated on census designated places (CDPs) level rather than census tract or block group. Therefore, the data was not spatially aligned with the other demographic data and not available for the entire county.

Still, the team mapped the prevalence of chronic illness across the county to subjectively analyze its relationship to extreme heat. As demonstrated by Figure 16 and appendix B, the area of North Sarasota had high incidences of all health hazards; for asthma and stroke, it is one of the highest areas overall. The areas near North Port, while not showing as consistently high case incidents as North Sarasota, still saw among the highest numbers of diabetes, Chronic Obstructive Pulmonary Disease (COPD), coronary heart disease (CHD), stroke, and high blood pressure (HBP). The health problem with the highest overall incidence rates was HBP, which largely clustered in the southern portion of the county around Venice Beach and Englewood and reached as high as just under 50 cases. The health issue with the smallest maximum number of cases was stroke, which capped out at 6.3 on average and were prevalent in the southern and central parts of the county and in North Sarasota and North Port. Since this data comes from hospital records, and hospitals are largely clustered where people live (hence the spatial bias towards the coast and the northwest), there is an amount

of uncertainty when it comes to where the people going to the hospitals are coming from and what number those who could not or would not make the trip made up of each; however, overall, these numbers depict a fairly robust picture of health problems within Sarasota County.

4.2.3 Demographic Data

There are a few limitations for the demographic data: the first is that the information, while it is US Census data, is from the American Community Survey (ACS), and therefore exists as estimates stretched from 2018 to 2022. Therefore, while the data has a degree of robustness promised by the magnitude of organization inherent to the Census Bureau, there is still a margin of error present on account of being estimates. Additionally, two of the demographic files presented issues at points that must be acknowledged. The first issue involved the 'race' demographic, which itself was created for use in ArcGIS Pro by combining ACS statistics from two Census tables, one of which detailed populations that were or were not White/Latin American, and one that specifically designated populations that were/were not Latin American. Because the former table grouped Caucasian and Latin American groups, and because, for the purpose of the analysis, the numbers specifically for overall White versus Non-White groups needed to be ascertained, the population values for Latin Americans were taken from the second ACS table for the same period and subtracted from the total. The issue is that the margins of error for the first table do not match up with the second (since they were averaged as separate data), and therefore the final numbers used in ArcGIS Pro have a higher margin of error than many of their demographic counterparts, despite all being from the same survey during the same period.

Additionally, the data corresponding to language proficiency would not run in ModelBuilder, possibly because many of the values were small enough as to fall within their own margins of error; trying to change the polygons into rasters for this data resulted in a blank file, despite multiple redownloading and reformatting attempts. Because of this, the demographic data for language proficiency is not included in the consideration process for the Heat Vulnerability model created in ModelBuilder; however, this absence is in part negated by its inclusion as part of the PCA process for heat exposure.

4.3 Future Work and Recommendations

There are several ways in which future research could improve the team's work. For one, a different evapotranspiration dataset could be used that incorporates more measurements to generate a model input closer to average conditions. This would improve the accuracy of the InVEST model. Additionally, high-resolution microclimate models like Envi-MET or SOlar and LongWave Environmental Irradiance Geometry model could be used to investigate air temperature variation in relation to LST. Future work could also examine the performance of higher resolution datasets.

Future work should also investigate potential mitigation methods to address extreme heat. Though the team's research indicated that tree canopy cover was negatively associated with LST, which could allow for mitigation through tree planting, this study did not touch on the specifics of what this would look like or how effective it would be. Other potential avenues of mitigation include creating publicly available information about extreme heat in the county, monitoring heat mitigation priority areas using low-cost temperature sensors, placing cooling centers in vulnerable communities, and increasing albedo by installing light-colored roofs.

4.4 Feasibility for Partner Use

In addition to directly incorporating the team's analysis into decision-making around heat mitigation, Sarasota County Sustainability could implement several of the team's methods into future assessment of urban heat. LST and cooling capacity should continue to be monitored as development changes land cover type in the county and climate change further increases average temperatures. The methods outlined in this paper could be implemented by Sarasota County Sustainability to study these changes for years into the future.

5. Conclusions

Based on NASA Earth Observation data, land surface temperatures across Sarasota County varies widely especially during Summertime. For Sarasota County, the highest temperatures typically occur in the more urbanized western portion of the county, and the lowest temperatures occur in the less developed portion of the county. Maps produced from the project indicate that LST values per county differ by as much as 55° F, largely according to land cover type. Similarly, the ability of the land to dissipate heat and cool itself, as determined by the team's modeled cooling capacity index, varies significantly, with vegetated land. The latter is more able to dispel much more heat than the impervious non-vegetated surfaces of the developed cities. Tree canopy cover is negatively associated with high temperatures within the county and positively associated with the cooling capacity index, indicating that tree planting in high-risk areas presents a potential mitigation measure against extreme heat through lowering the temperature and providing shade for human inhabitants.

Heat sensitive populations, vulnerable to the continued strain of living and working in high-heat regions, often overlap with the high temperatures present in the county. Using a demographic model of heat vulnerability, a principal component analysis of demographic and environmental variables, and the distribution of extreme heat in the county, the team identified three geographic areas of particular importance for heat related issues in Sarasota County, i.e. North Sarasota, Venice, and Northport, for consideration of future heat mitigation measures.

6. Acknowledgements

The team would like to thank the partners, science advisors, and center lead for giving project input and constructive feedback throughout the Spring 2024 term from January 22nd to March 29th, 2024.

- **Partners:** Alia Garrett, Gary Schells, and Anna Leavitt (Sarasota County Government – UF/IFAS Extension)
- **Science Advisors:** Dr. Marguerite Madden (University of Georgia) and Joseph Spruce (Langley Research Center, Analytical Mechanics and Associates)
- **Center Lead**: Megan Rich (NASA DEVELOP at Georgia-Athens)
- **Coding Guidance**: Dr. Kenton Ross (NASA DEVELOP Program Manager)
- **Deliverable Feedback**: Laramie Plott (NASA DEVELOP Senior Fellow)

Any opinions, findings, and conclusions or recommendations expressed in this material are those of the author(s) and do not necessarily reflect the views of the National Aeronautics and Space Administration.

This material is based upon work supported by NASA through contract 80LARC23FA024.

7. Glossary

Albedo: The fraction of incoming light that is reflected by a surface.

Cooling Capacity Index: An output index of the InVEST suite that represents cooling effect of green spaces.

Earth observations: Satellite, airborne, and in-situ sensors that collect information about the Earth's physical, chemical, and biological systems over space and time.

ECOsystem Spaceborne Thermal Radiometer on Space Station (ECOSTRESS): A satellite mission on board the International Space Station (ISS) which aims to measure how ecosystems respond to environmental changes.

Eigenvalues: A constant, scalar value which contributes to the characterization of a matrix of linear equations.

Evapotranspiration (ET): A cumulative process in which water is transferred from the land surface to the atmosphere through evaporation and transpiration.

Heat Mitigation Priority: Overall cumulative heat vulnerability based on three model's output.

Integrated Valuation of Ecosystem Services and Tradeoffs (InVEST): a suite of free, open-source models used to map and interpret natural goods and services that benefit human society.

Landsat 8: Earth observation satellite launched in 2013 that includes the Operational Land Imager (OLI) Sensor and Thermal Infrared Sensor (TIRS).

Landsat 9: Earth observation satellite launched in 2021 that includes the Operational Land Imager (OLI-2) Sensor and Thermal Infrared Sensor (TIRS-2).

Urban Heat Island (UHI): A developed area that is significantly warmer than the surrounding undeveloped land due to how much different surfaces absorb and retain heat.

8. References

Allen, R.G., Pereira, L.S., Raes, D., & Smith, M. (1998). Crop Evapotranspiration-Guidelines for computing crop water requirements- FAO Irrigation and drainage paper 56. *FAO, Rome*, *300*(9). D05109. https://www.fao.org/3/X0490E/x0490e0b.htm#TopOfPage.

Bao, J., Li, X., & Yu, C. (2015). The construction and validation of the heat vulnerability index, a review. *International Journal of Environmental Research and Public Health*, *12*(7): 7220-7234. https://doi.org/10.3390/ijerph120707220.

Benmarhnia, T., Deguen, S., Kaufman, J., & Smargiassi, A. (2015). Vulnerability to Heat-related Mortality: A Systematic Review, Meta-analysis, and Meta-regression Analysis. *Epidemiology, 26*(6): 781-793. https://doi.org/10.1097/ede.0000000000000375.

Bouchama, A. (2004). The 2003 European heat wave. *Intensive Care Medicine*, *30*: 1-3. https://doi.org/10.1007/s00134-003-2062-y

Conlon, K. C., Mallen, E., Gronlund, C. J., Berrocal, V. J., Larsen, L., & O'Neill, M. S. (2020). Mapping human vulnerability to extreme heat: A critical assessment of heat vulnerability indices created using principal components analysis. *Environmental health perspectives*, *128*(9), 097001. https://doi.org/10.1289/EHP4030.

Faurie, C., Varghese, B. M., Liu, J., & Bi, P. (2022). Association between high temperature and heatwaves with heat-related illnesses: A systematic review and meta-analysis. S*cience of The Total Environment*, 852, 158332. https://doi.org/10.1016/j.scitotenv.2022.158332.

Ghosh, R., Kirschner, R., Monaghan, R., & Mukherjee, R. (2022). *Quantifying and Mapping Urban Heat to Inform Equitable and Sustainable Urban Planning Initiatives in Wichita, Kansas*. NASA DEVELOP Technical Report. https://ntrs.nasa.gov/citations/20220018645.

Hansen, A., Bi, L., Saniotis, A., & Nitschke, M. (2013). Vulnerability to extreme heat and climate change: is ethnicity a factor?. *Global Health Action. 6*(1): 21364. https://doi.org/10.3402/gha.v6i0.21364.

Harlan, S. L., Chowell, G., Yang, S., Petitti, D. B., Butler, E. J. M., Ruddell, B. L., & Ruddell, D. (2014). Heat-Related deaths in hot Cities: Estimates of human tolerance to high temperature thresholds.

International Journal of Environmental Research and Public Health, *11*(3), 3304–3326. https://doi.org/10.3390/ijerph110303304.

Holloway, W. P., Eichelmann, R., Murer, P., Newell, R., O'Connell, C. (2021). *Identifying Urban Heat Mitigation Strategies for Climate Adaptation Planning in Fairfax County, Virginia.* NASA DEVELOP Technical Report. https://ntrs.nasa.gov/citations/20210021471

Hook, S. & Hulley, G. (2019). *ECOSTRESS land surface temperature and emissivity daily L2 global 70 m V001 [Data set]*. NASA EOSDIS Land Processes DAAC. https://doi.org/10.5067/ECOSTRESS/ECO2LSTE.001

Liang, S. (2001). Narrowband to broadband conversions of land surface albedo I: Algorithms. *Remote sensing of environment*, *76*(2), 213-238. https://doi.org/10.1016/S0034-4257(00)00205-4.

Méndez-Lázaro, P., Muller-Karger, F. E., Otis, D., McCarthy, M. J., & Rodríguez, E. (2018). A heat vulnerability index to improve urban public health management in San Juan, Puerto Rico. *International Journal of Biometeorology,* 62, 709-722. https://doi.org/10.1007/s00484-017-1319-z.

Natural Capital Project. (2024). InVEST 3.14.1. Stanford University, University of Minnesota, Chinese Academy of Sciences, The Nature Conservancy, World Wildlife Fund, Stockholm Resilience Centre and the Royal Swedish Academy of Sciences. https://naturalcapitalproject.stanford.edu/software/invest.

National Aeronautics and Space Administration. (2019, November 18). Albedo values. My NASA Data. https://mynasadata.larc.nasa.gov/basic-page/albedo-values.

National Oceanic and Atmospheric Administration. (2022, March 3). NOAA Online Weather Data. https://www.weather.gov/wrh/Climate?wfo=tbw.

Nuruzzaman, M. (2015). Urban Heat Island: Causes, Effects and Mitigation Measures - A Review. *International Journal of Environmental Monitoring and Analysis. 3*(2): 67-73. https://doi.org/10.11648/j.ijema.20150302.15

Reid, C. E., O'neill, M. S., Gronlund, C. J., Brines, S. J., Brown, D. G., Diez-Roux, A. V., & Schwartz, J. (2009). Mapping community determinants of heat vulnerability. *Environmental health perspectives*, *117*(11), 1730-1736. https://doi.org/10.1289/ehp.0900683.

Semenza, J. C., Rubin, C. H., Falter, K. H., Selanikio, J. D., Flanders, W. D., Howe, H. L., & Wilhelm, J. L. (1996). Heat-related deaths during the July 1995 heat wave in Chicago. N*ew England Journal of Medicine*, *335*(2): 84-90. https://doi.org/10.1056/nejm199607113350203.

Smith, R. B. (2010). The heat budget of the earth's surface deduced from space. *Yale University Center for Earth Observation: New Haven, CT, USA*. https://yceo.yale.edu/how-convert-landsat-dns-albedo

Union of Concerned Scientists. (2019). *Killer Heat Interactive Tool.* https://www.ucsusa.org/resources/killer-heat-interactive-tool.

U.S. Geological Survey. (n.d.) USGS EROS Archive – Landsat Archives – Landsat 8-9 OLI/TIRS Collection 2 Level-2 Science Products. https://doi.org/10.5066/P9OGBGM6.

Walechka, J., Bils, T., Greenler, K., Sabrin, S., & Scarmuzza, J. (2021). *Utilizing NASA Earth Observations to Identify Environmental and Social Drivers of Urban Heat Vulnerability and Model Urban Cooling Interventions in*

Yonkers, New York. NASA DEVELOP Technical Report. https://ntrs.nasa.gov/citations/20210024373.

Yardley, J. E., Sigal, R. J., & Kenny, G. P. (2011). Heat health planning: The importance of social and community factors. *Global Environmental Change*, *21*(2), 670–679. https://doi.org/10.1016/j.gloenvcha.2010.11.010.

Zawadzka, J. E., Harris, J. A., & Corstanje, R. (2021). Assessment of heat mitigation capacity of urban greenspaces with the use of In-VEST urban cooling model, verified with day-time land surface temperature data. *Landscape and Urban Planning, 214*, 104163. https://doi.org/10.1016/j.landurbplan.2021.104163.

9. Appendices

Appendix A: Principal Component Analysis

Table A
Heat Exposure Variables Principal Component Loadings

	PC1	PC2	PC3	PC4
% of Impervious Surfaces	**0.922**	-0.052	0.174	0.091
Daytime LST	**0.887**	-0.169	0.213	0.104
Albedo	**0.876**	0.161	0.085	0.105
Nighttime LST	0.580	0.108	**-0.418**	-0.211
% of Canopy Cover	**-0.580**	-0.276	-0.002	-0.027
% Living Alone	0.569	0.525	0.239	-0.010
Total Population	**-0.473**	**-0.349**	0.320	-0.067
% of People with Disability	0.008	**0.862**	-0.015	-0.024
% of Age 65 years old and over	0.173	**0.763**	**-0.468**	-0.247
% Not in Labor Workforce	0.106	0.751	**-0.398**	-0.258
% Non-Caucasian/White	0.017	-0.197	0.746	0.196
% Below Poverty Line	0.273	-0.198	0.634	0.187
% Without Car	0.284	0.440	0.628	0.019
% Not a Citizen	0.128	-0.041	0.092	**0.864**
% Limited English Proficiency	0.072	-0.088	0.181	**0.801**
% Without Health Insurance	-0.084	**-0.291**	0.535	0.551
Proportion Variance	0.24	0.17	0.15	0.12
Cumulative Variance	0.24	0.42	0.57	0.69

Appendix B: CDP locations for health data

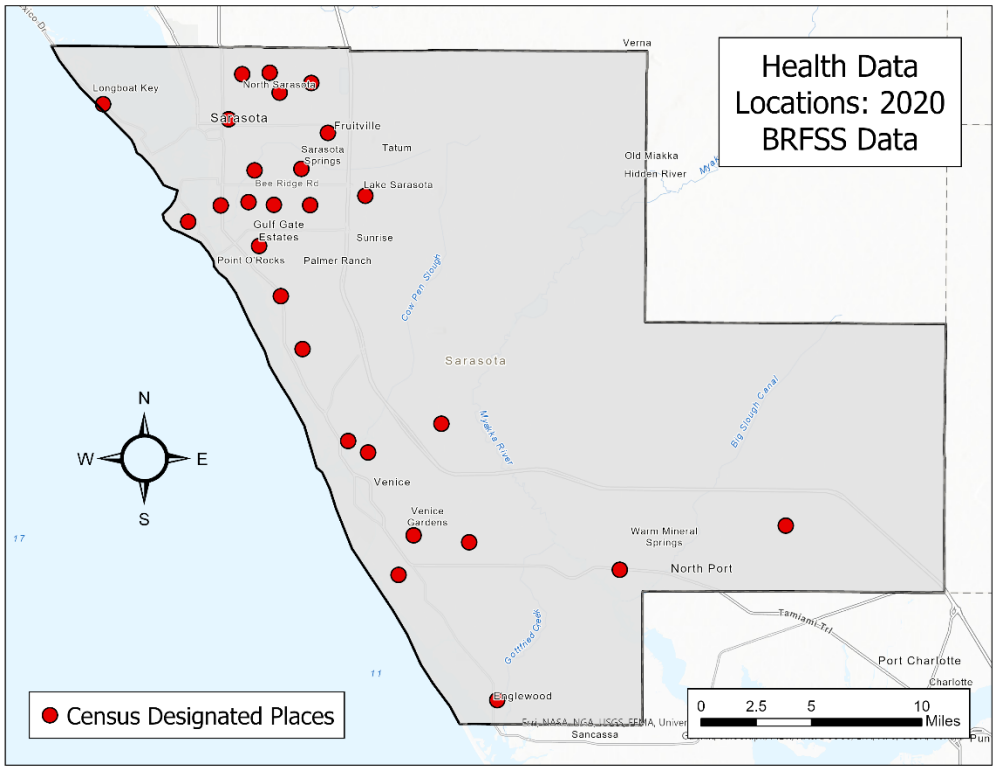

Figure B. Spatial distribution of health data locations.

Table B

List of Sarasota County Census-designated Places (CDPs)

Sarasota County Census-designated Places			
Venice	Kensington Park	Pinecraft	The Meadows
Longboat Key	Lake Sarasota	Plantation	Vamo
North Port	Lakewood Ranch	Port Charlotte	Venice Gardens
Sarasota	Laurel	Ridge Wood Heights	Warm Mineral Springs
Bee Ridge	Manasota Key	Sarasota Springs	
Desoto Acres	Nokomis	Siesta Key	
Desoto Lakes	North Sarasota	Southgate	
Englewood	Old Miakka	South Gate Ridge	
Fruitville	Osprey	South Sarasota	
Gulf Gate	Palmer Ranch	South Venice	

Appendix C: Individual demographic data breakdown by variable

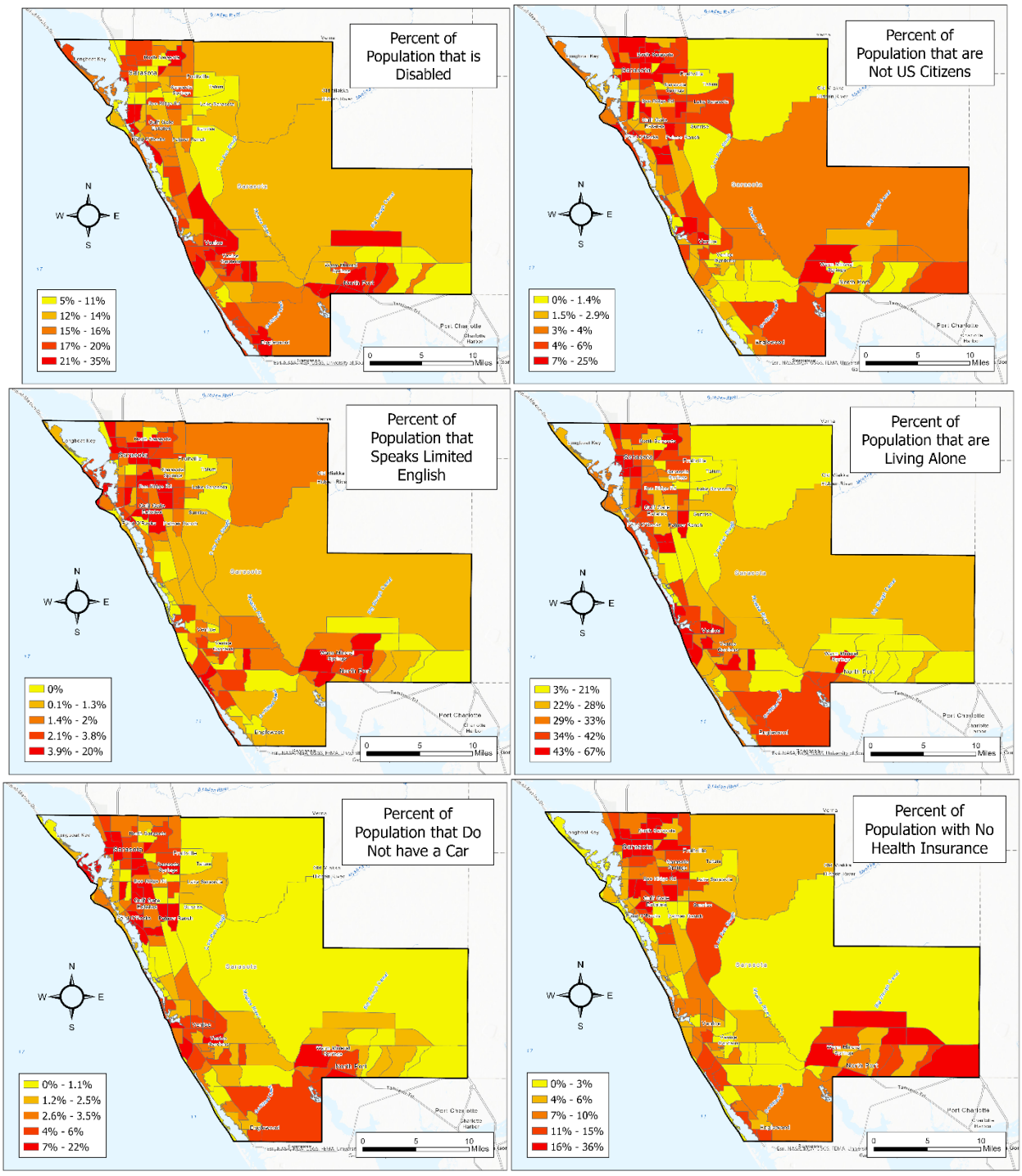

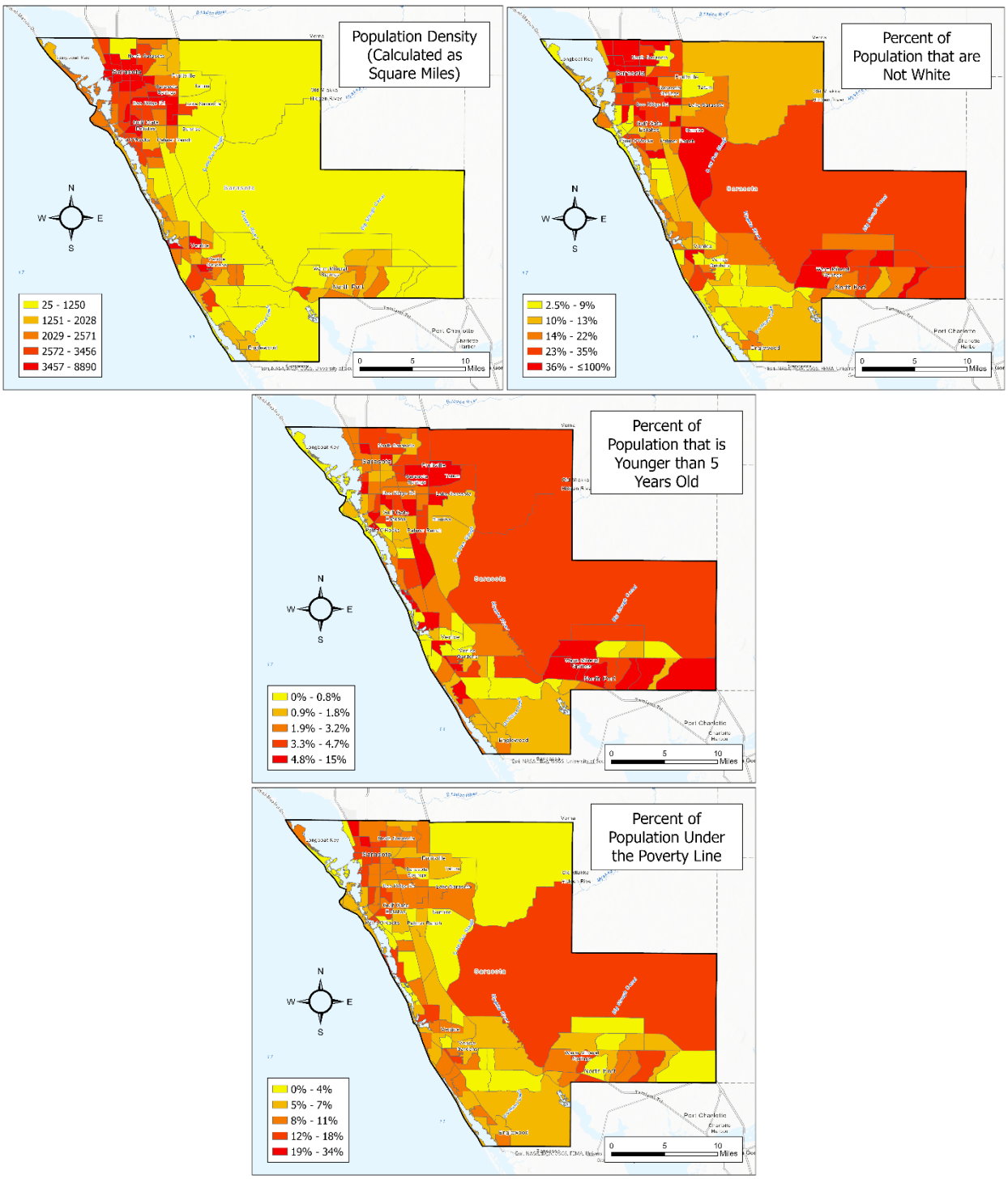

Figure C. 10 other ACS Socioeconomic variables across Sarasota County, FL (by census tracts).

Appendix D: ArcGIS ModelBuilder step-by-step process

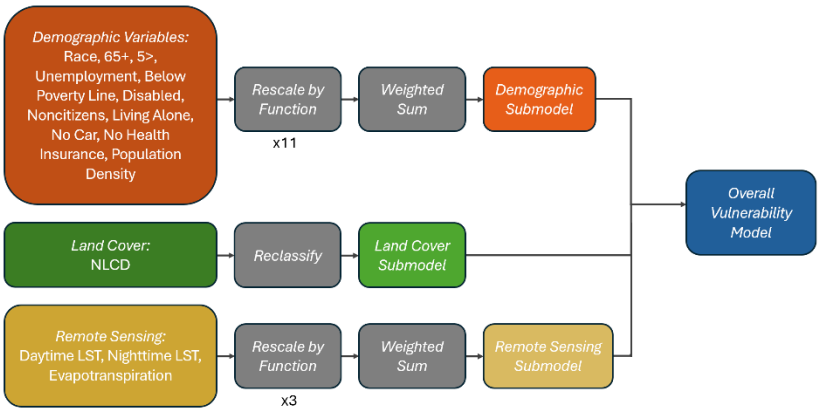

Figure D. Layout of arrangement of rasters and shapefiles in ModelBuilder.